DESY 13–159 ISSN 0418-9833
September 2013

Inclusive J/ψ and $\psi(2S)$ production from b-hadron decay in $p\bar{p}$ and pp collisions

Paolo Bolzoni,* Bernd A. Kniehl,† and Gustav Kramer‡
II. Institut für Theoretische Physik, Universität Hamburg, Luruper Chaussee 149, 22761 Hamburg, Germany

(Dated: September 16, 2013)

Abstract

We study the inclusive production of J/ψ and $\psi(2S)$ mesons originating from the decays of bottom-flavored hadrons produced in $p\bar{p}$ collisions at the Fermilab Tevatron and in pp collisions at the CERN LHC. We work at next-to-leading order in the general-mass variable-flavor-number scheme (GM-VFNS) implemented with nonperturbative fragmentation functions fitted to e^+e^- data of inclusive b-hadron production exploiting their universality. The three-momentum distributions of the charmonia are extracted from B-decay data in the framework of nonrelativistic-QCD factorization. Comparing the theoretical predictions thus obtained with transverse-momentum distributions measured by the CDF II, ALICE, ATLAS, CMS, and LHCb Collaborations, we find excellent overall agreement as for both absolute normalization and lineshape, which provides a nontrivial test of the GM-VFNS over wide ranges of center-of-mass energy, transverse momentum, and rapidity.

PACS numbers: 13.25.Hw, 13.85.Ni, 13.87.Fh, 14.40.Pq

*Electronic address: paolo.bolzoni@desy.de
†Electronic address: kniehl@desy.de
‡Electronic address: gustav.kramer@desy.de

I. INTRODUCTION

Already several years ago, the CDF Collaboration at the Fermilab Tevatron extracted individual cross sections for the inclusive production of J/ψ and $\psi(2S)$ mesons originating from decays of B mesons and other b hadrons [1]. The cross sections were differential in the charmonium transverse momentum (p_T) and covered the range 5 GeV $< p_T <$ 20 GeV. Next-to-leading-order (NLO) predictions provided by two of us [2] were found to nicely reproduce these measurements over the whole p_T range. The calculation had two ingredients, the inclusive production cross section of the process $p\bar{p} \to B + X$, differential in p_T and rapidity (y), and the partial widths of the inclusive decays $B \to J/\psi + X$ and $B \to \psi(2S) + X$ as functions of the J/ψ and $\psi(2S)$ momentum fractions, respectively. The first ingredient was calculated at NLO in the zero-mass variable-flavor-number scheme (ZM-VFNS) [3], which corresponds to the conventional parton-model approach endowed with nonperturbative fragmentation function (FFs) for the transition $b \to B$, as described in Ref. [4]. In this approach, the b quark is included among the incoming partons, along with the u, d, s, and c quarks and the gluon g, leading to additional contributions. Previous CDF measurements of the inclusive B^+/B^0 production cross section at center-of-mass energy $\sqrt{s} = 1.8$ TeV [5] were found to be in satisfactory agreement with such NLO ZM-VFNS predictions, provided that realistic FFs are adopted [4]. The second ingredient was obtained in the framework of the parton model in combination with nonrelativistic-QCD (NRQCD) factorization [6] by applying the approach of Palmer, Paschos, and Soldan [7] to the $B \to J/\psi + X$ and $B \to \psi(2S) + X$ decay distributions measured by the the CLEO Collaboration [8]. Subsequently, the inclusive cross section of nonprompt J/ψ hadroproduction at Tevatron energies was also computed in the FONLL and MC@NLO approaches [9].

The CDF Collaboration repeated their measurement of the inclusive cross section of nonprompt J/ψ [10] and $\psi(2S)$ [11] hadroproduction in run II (CDF II) at $\sqrt{s} = 1.96$ TeV with a much higher accuracy reaching also below $p_T = 5$ GeV. Recently, all four LHC experiments, CMS [12, 13], LHCb [14, 15], ATLAS [16], and ALICE [17], released their measurements of the corresponding J/ψ [12–14, 16, 17], and $\psi(2S)$ [13, 15] observables in pp collisions with $\sqrt{s} = 7$ TeV. These data offer the opportunity to test the b-hadron production models in a new energy regime using the common decay channels to J/ψ and $\psi(2S)$ mesons.

In this paper, we present a new analysis of the inclusive cross sections of nonprompt J/ψ and $\psi(2S)$ hadroproduction with theoretical input improved relative to our previous work [2]. Specifically, the ZM-VFNS is replaced by the general-mass variable-flavor-number scheme (GM-VFNS), which has been elaborated in recent years [18–20]. Furthermore, we adopt an updated $b \to B$ FF extracted [19] from more recent data of $e^+e^- \to B + X$ at the Z-boson resonance [21–23] as well as advanced parton distribution functions (PDFs) [24]. On the other hand, the formalism for the description of the inclusive decays $B \to J/\psi + X$ and $B \to \psi(2S) + X$ is taken over from Ref. [2] without changes, since it is still quite appropriate. To gain confidence in the reliability of our NLO treatment of inclusive B-meson production, we performed comparisons [19, 20] with CDF II data from $p\bar{p}$ collisions at $\sqrt{s} = 1.96$ TeV [10] at and with CMS data from pp collisions at $\sqrt{s} = 7$ TeV [25], to find very good agreement, in particular for larger p_T values. In Ref. [2], the polarization of the J/ψ and $\psi(2S)$ mesons from b-hadron decay was not considered. According to Ref. [26], it is small in both cases.

This paper is organized as follows. In Sec. II, we briefly describe our theoretical framework and choice of inputs, pointing towards the appropriate references. In Sec. III, we compare our NLO GM-VFNS predictions for the inclusive cross sections of nonprompt J/ψ and $\psi(2S)$ hadroproduction with recent measurements at the Tevatron [10, 11] and the LHC [12–17]. Section IV contains our conclusions.

II. SETUP AND INPUT

The technical details of the GM-VFNS framework and results obtained from it were previously presented in Refs. [18–20]. Here, we only describe our choice of input for the numerical analysis of nonprompt J/ψ and $\psi(2S)$ hadroproduction. We use the set CTEQ6.6 [24] of proton PDFs as implemented in the LHAPDF library [27]. This PDF set was obtained in a general-mass scheme using the input values $m_c = 1.3$ GeV, $m_b = 4.5$ GeV, and $\alpha_s(m_Z) = 0.118$, and taking the starting scale of the b-quark PDF to be $\mu_0 = m_b$. We employ the nonperturbative B-meson FFs determined in Ref. [19] by fitting experimental data on the inclusive cross section of B-meson production in e^+e^- annihilation taken by the ALEPH [21] and OPAL [22] Collaborations at CERN LEP1 and by the SLD Collaboration [23] at SLAC SLC. These FFs supersede the ones extracted from OPAL data [28] in Ref. [4]. All these data were taken on the Z-boson resonance, so that finite-m_b effects can safely be neglected. In Ref. [19], the asymptotic scale parameter was taken to be $\Lambda^{(5)}_{\overline{\rm MS}} = 0.227$ GeV at NLO, the factorization and renormalization scales were identified with the Z-boson mass, $\mu_F = \mu_R = m_Z$, and the starting scale of the $b \to B$ FF was chosen to be $\mu_0 = m_b$ in accordance with Ref. [24], while the $q, g \to B$ FFs, where $q = u, d, s, c$, were assumed to vanish at $\mu_F = \mu_0$. We select the FF set implemented with the simple power ansatz, which yielded the best fit, as may be seen in Fig. 1 of Ref. [19]. The OPAL [22] and SLD [23] data included all the b-hadron final states, i.e. all the B mesons, $B^\pm$, $B^0/\bar{B}^0$, and $B^0_s/\bar{B}^0_s$, and the b baryons, such as the Λ^0_b baryon, while, in the ALEPH analysis [21], only final states with identified $B^\pm$ and $B^0/\bar{B}^0$ mesons were taken into account. In Ref. [19], the FFs of all b hadrons were assumed to have the same shape. In addition, we shall assume here that all the b hadrons have the same branching fractions and decay distributions into J/ψ and $\psi(2S)$ mesons as the B mesons. Differences only arise from the different b-quark to b-hadron branching fractions, which we adopt from the Particle Data Group (PDG) [29]. For example, the $B^0/\bar{B}^0$-meson contribution is to be multiplied by $100\%/40.1\% = 2.49$. For simplicity, we take the initial- and final-state factorization scales, entering the PDFs and FFs, respectively, to have the same value μ_F. We choose μ_F and the renormalization scale μ_R, at which α_s is evaluated, to be $\mu_F = \xi_F m_T$ and $\mu_R = \xi_R m_T$, respectively, where $m_T = \sqrt{p_T^2 + m_b^2}$ with p_T being the transverse momentum of the J/ψ or $\psi(2S)$ mesons, and independently vary the parameters ξ_F and ξ_R about their default values $\xi_F = \xi_R = 1$ up and down by a factor of two under the restriction $1/2 \leq \xi_R/\xi_F \leq 2$ to estimate the theoretical uncertainty due to the lack of knowledge of beyond-NLO corrections. In fact, scale variations constitute the overwhelming source of theoretical uncertainties in our predictions. We may, therefore, neglect the uncertainties in the PDFs and m_b. For consistency with Ref. [24], we use $m_b = 4.5$ GeV throughout this work. As in Ref. [2], we employ an effective FF for the transition of parton i via the B meson to the J/ψ (or $\psi(2S)$) meson, which is calculated as the convolution

$$D_{i\to J/\psi}(x, \mu_F) = \int_x^1 \frac{dz}{z} D_{i\to B}\left(\frac{x}{z}, \mu_F\right) \frac{1}{\Gamma_B} \frac{d\Gamma}{dz}(z, P_B), \tag{1}$$

where $D_{i\to B}(y, \mu_F)$ are the nonperturbative FFs at B-to-i longitudinal-momentum fraction y and factorization scale μ_F, as determined in Ref. [19], Γ_B is the B-meson total decay width, and $d\Gamma(z, P_B)/dz$ is the $B \to J/\psi$ decay distribution differential in the J/ψ-to-

B longitudinal-momentum fraction z, as given in Eqs. (3.12) or (3.16) of Ref. [2]. For given J/ψ transverse momentum p_T and rapidity y, the modulus of the B three-momentum $\mathbf{P_B}$ is $P_B = |\mathbf{P_B}| = \sqrt{p_T^2 + m_T^2 \sinh^2 y}/z$. We use the B^+/B^0 average mass value $M_B = 5.279$ GeV and average lifetime value $\tau_B = 1.61$ ps. In Ref. [2], the decay distribution $d\Gamma/dk'_L$ in the component k'_L of the J/ψ three-momentum parallel to $\mathbf{P_B}$ is obtained by integrating the general formula, given in Eq. (3.4) of Ref. [2], over the orthogonal three-momentum components. This leads to the quantity $d\Gamma(z, P_B)/dz$ appearing in Eq. (1), where $z = k'_L/P_B$. It depends on the structure function $f(x)$ of the $b \to B$ transition, the element V_{cb} of the Cabibbo-Kobayashi-Maskawa matrix, and the coefficients a and b arising from NRQCD. In Ref. [2], these coefficients were fitted to the branching fraction and the momentum distribution of the decay $B \to J/\psi + X$ measured by the CLEO Collaboration [8]. The latter agrees very well with the BaBar measurement [30], which was not yet available for the fit [2]. Besides direct J/ψ production via $B \to J/\psi + X$, we also included the feed-down contributions from $B \to \chi_{cJ} + X$ with $J = 0, 1, 2$ followed by $\chi_{cJ} \to J/\psi + \gamma$ and from $B \to \psi(2S) + X$ followed by $\psi(2S) \to J/\psi + X$. The branching fraction of the direct channel was found to be 0.80%, while those of the cascades via the χ_{cJ} and $\psi(2S)$ mesons were found to be 0.13% and 0.19%, respectively. Further details may be found in Ref. [2]. Since the appearance of the CLEO paper [8], some of these input values have changed slightly. However the most relevant result, namely the total $B \to J/\psi + X$ branching fraction, goes unchanged, if up-to-date input data from the PDG [29] is used. To facilitate the calculation, we evaluate $d\Gamma(z, P_B)/dz$ using its asymptotic expression, obtained from Eq. (3.14) in Ref. [2] in the limit $P_B \gg M_B$. This approximation deviates from the exact result by less than 11% and 5% for $P_B = 10$ GeV and 20 GeV, respectively. In most of our applications, we have $P_B > 20$ GeV.

III. RESULTS

We are now in a position to present our numerical analysis. In Figs. 1 and 2, we compare measurements of the inclusive cross sections of nonprompt J/ψ [10, 12–14, 16, 17] and $\psi(2S)$ [11, 13, 15] hadroproduction, respectively, with our NLO GM-VFNS predictions evaluated as described in Sec. II. The experimental data come as the cross section distributions $d\sigma/dp_T$ integrated over $2.0 < y < 4.5$ [15], $\mathrm{Br}\times d\sigma/dp_T$ integrated over $|y| < 0.6$ [10, 11], $d^2\sigma/(dp_T dy)$

[14, 17], and Br $\times\, d^2\sigma/(dp_T dy)$ [12, 16], where Br stands for the branching fractions of the decays $J/\psi \to \mu^+\mu^-$ and $\psi(2S) \to \mu^+\mu^-$, for which we adopt the values Br $= 5.93\%$ and 0.77%, respectively, from Ref. [29]. Besides the default predictions with $\xi_F = \xi_R = 1$, we also present error bands encompassed between the minimum and maximum values obtained by the variations of ξ_F and ξ_R as explained in Sec. II. The slight changes of slope in the lower bounds at about $p_T = 8$ GeV reflect the fact that the partonic subprocesses initiated by a b quark are turned off by the b-quark PDF as the threshold at $\mu_F = m_b$ is reached.

We now take a closer look at Fig. 1. From Fig. 1(a), we observe that the CDF II data points [10] are all contained within the theoretical-error band, exhibiting a slight tendency to undershoot the default prediction at small and large p_T values. We do not consider data available in the range $1.25 < p_T < 3.0$ GeV [10], where our theoretical predictions are less reliable. The CMS data [12, 13] shown in Figs. 1(b)–(f) are sampled in the five y bins $|y| < 0.9$, $0.9 < |y| < 1.2$, $1.2 < |y| < 1.6$, $1.6 < |y| < 2.1$, and $2.1 < |y| < 2.4$, respectively, and cover different p_T ranges. The measurement in the most central rapidity bin reaches out through $p_T = 70$ GeV. The experimental errors shown are obtained by summing quadratically the statistical, systematic, and luminosity-related errors. The agreement between experiment and theory is rather satisfactory, except for the largest-p_T bins, where the measurements including their errors tend to lie underneath the theory bands. The LHCb data [14] displayed in Figs. 1(g)–(k) refer to five y bins of equal widths in the range $2.0 < y < 4.5$ covering different p_T ranges, the widest being 2.0 GeV $< p_T <$ 14.0 GeV. With one exception, all the central data points fall inside the theory bands. The data points tend to undershoot the default predictions, the more so at small p_T values. The ATLAS data [16] included in Figs. 1(l)–(o) are grouped in the four y bins $|y| < 0.75$, $0.75 < |y| < 1.5$, $1.5 < |y| < 2.0$, and $2.0 < |y| < 2.4$, respectively, and cover p_T values as large as 70 GeV. They agree very well with our NLO GM-VFNS predictions, being gathered within the theory bands, with the exception of the data points of largest p_T in each of Figs. 1(l), (m), and (o), which are slightly below. In fact, most of the data points even agree with our default predictions within the experimental errors. Very recently, the ALICE Collaboration reported their measurement of prompt and nonprompt J/ψ hadroproduction in Ref. [17]. There are four ALICE data points, in the kinematic range $p_T > 1.3$ GeV and $|y| < 0.9$, which may be extracted from Ref. [17] by multiplying the respective results for the inclusive cross section of prompt plus nonprompt J/ψ hadroproduction and the fraction of J/ψ mesons from b-hadron decays,

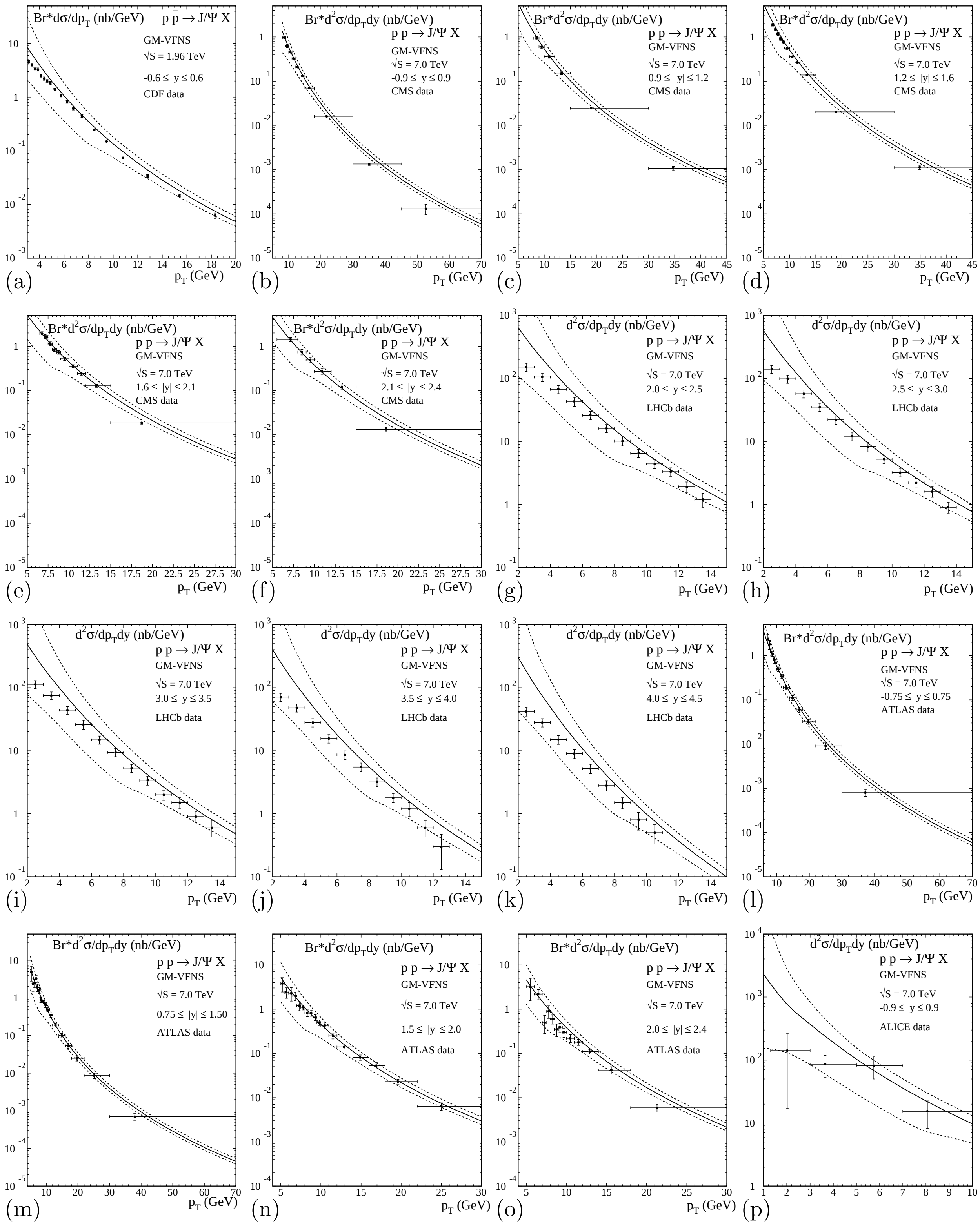

FIG. 1: The inclusive cross sections of nonprompt J/ψ hadroproduction measured by CDF II [10] in $p\bar{p}$ collisions at $\sqrt{s} = 1.96$ TeV and by CMS [12, 13], LHCb [14], ATLAS [16], and ALICE [17] in pp collisions at $\sqrt{s} = 7$ TeV are compared with NLO GM-VFNS predictions, whose default values and error bands are indicated by the solid and dashed lines, respectively.

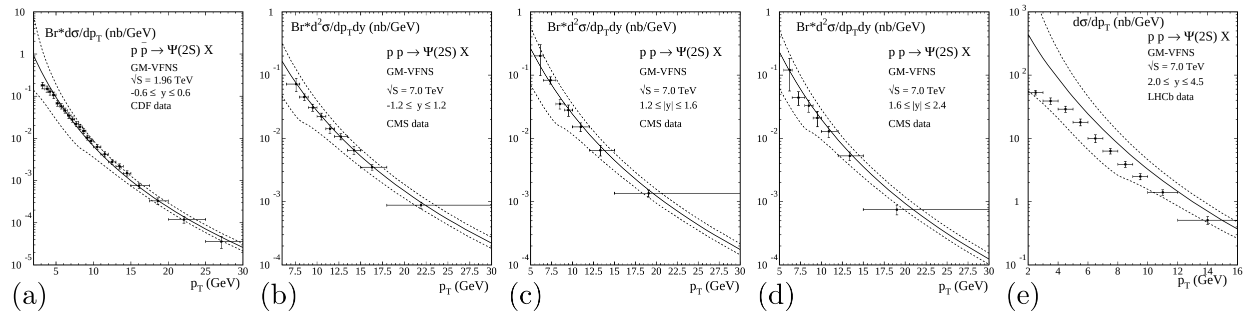

FIG. 2: The inclusive cross sections of nonprompt $\psi(2S)$ hadroproduction measured by CDF II [11] in $p\bar{p}$ collisions at $\sqrt{s} = 1.96$ TeV and by CMS [13] and LHCb [15] in pp collisions at $\sqrt{s} = 7$ TeV are compared with NLO GM-VFNS predictions, whose default values and error bands are indicated by the solid and dashed lines, respectively.

appropriately combining the experimental errors. All the four data points agree with our NLO GM-VFNS predictions within the theoretical uncertainties as may be seen in Fig. 1(p).

We now move on to Fig. 2. While nonprompt J/ψ production is also possible via the feed-down from heavier charmonia, nonprompt $\psi(2S)$ production proceeds only directly. The CDF II data [11], the CMS data [13] in the y bins $|y| < 1.2$, $1.2 < |y| < 1.6$, and $1.6 < |y| < 2.4$, and the LHCb data [15] are compared with our NLO GM-VFNS predictions in Figs. 2(a)–(e), respectively. The CDF II and CMS measurements, in the central regions of the detectors, reach out to $p_T = 30$ GeV, while the LHCb one, in the forward region, stops at $p_T = 16$ GeV. We conclude from Fig. 2 that all the experimental data points agree with our NLO GM-VFNS predictions within the theoretical uncertainties. With a few exceptions, all the CDF II and CMS data points agree with our default predictions within the experimental errors, while the LHCb data points consistently undershoot our default predictions.

IV. CONCLUSIONS

Motivated by recent measurements at the Tevatron [10, 11] and the LHC [12–17], we improved and updated our previous analysis of the inclusive cross sections of nonprompt J/ψ and $\psi(2S)$ hadroproduction [2] by adopting the GM-VFNS [18–20] and refreshing our inputs as described in Sec. II. In Sec. III, the transverse-momentum distributions measured by the CDF II [10, 11], CMS [12, 13], LHCb [14, 15], ATLAS [16], and ALICE [17] Collaborations were found to be very well described by our upgraded NLO predictions, as for both absolute normalization and lineshape. This constitutes a nontrivial test of the GM-VFNS over wide $\sqrt{s}$, p_T, and y ranges.

Acknowledgements

This work was supported by the German Federal Ministry for Education and Research BMBF through Grant No. 05H12GUE and by the German Research Foundation DFG through Grant No. KN 365/5-3.

[1] F. Abe *et al.* (CDF Collaboration), Phys. Rev. Lett. **79**, 572 (1997).

[2] B. A. Kniehl and G. Kramer, Phys. Rev. D **60**, 014006 (1999) [hep-ph/9901348].

[3] M. Cacciari and M. Greco, Nucl. Phys. **B421**, 530 (1994) [hep-ph/9311260]; M. Cacciari, M. Greco, B. A. Kniehl, M. Kramer, G. Kramer, and M. Spira, *ibid.* **B466**, 173 (1996) [hep-ph/9512246]; J. Binnewies, B. A. Kniehl, and G. Kramer, Z. Phys. C **76**, 677 (1997) [hep-ph/9702408]; B. A. Kniehl, G. Kramer, and M. Spira, *ibid.* **76**, 689 (1997) [hep-ph/9610267]; J. Binnewies, B. A. Kniehl, and G. Kramer, Phys. Rev. D **58**, 014014 (1998) [hep-ph/9712482].

[4] J. Binnewies, B. A. Kniehl, and G. Kramer, Phys. Rev. D **58**, 034016 (1998) [hep-ph/9802231]; B. A. Kniehl, in *Proceedings of the 14th Topical Conference on Hadron Collider Physics (Hadron Collider Physics 2002)*, Karlsruhe, Germany, 29 September–4 October 2002, edited by M. Erdmann and Th. Müller (Springer, Berlin, 2003), p. 161 [hep-ph/0211008].

[5] A. Laasanen *et al.* (CDF Collaboration), Report Nos. FERMILAB-Conf-96/198-E and CDF/PUB/BOTTOM/PUBLIC/3759 (1996), contributed to *28th International Conference on High Energy Physics (ICHEP '96)*, Warsaw, Poland, 25–31 July 1996.

[6] G. T. Bodwin, E. Braaten, and G. P. Lepage, Phys. Rev. D **51**, 1125 (1995); **55**, 5853(E) (1997) [hep-ph/9407339].

[7] W. F. Palmer, E. A. Paschos, and P. H. Soldan, Phys. Rev. D **56**, 5794 (1997) [hep-ph/9701328].

[8] R. Balest *et al.* (CLEO Collaboration), Phys. Rev. D **52**, 2661 (1995).

[9] M. Cacciari, S. Frixione, M. L. Mangano, P. Nason, and G. Ridolfi, J. High Energy Phys. 07 (2004) 033 [hep-ph/0312132].

[10] D. Acosta *et al.* (CDF Collaboration), Phys. Rev. D **71**, 032001 (2005) [hep-ex/0412071].

[11] T. Aaltonen *et al.* (CDF Collaboration), Phys. Rev. D **80**, 031103(R) (2009) [arXiv:0905.1982 [hep-ex]].

[12] V. Khachatryan *et al.* (CMS Collaboration), Eur. Phys. J. C **71**, 1575 (2011) [arXiv:1011.4193 [hep-ex]].

[13] S. Chatrchyan *et al.* (CMS Collaboration), J. High Energy Phys. 02 (2012) 011 [arXiv:1111.1557 [hep-ex]].

[14] R. Aaij *et al.* (LHCb Collaboration), Eur. Phys. J. C **71**, 1645 (2011) [arXiv:1103.0423 [hep-ex]].

[15] R. Aaij *et al.* (LHCb Collaboration), Eur. Phys. J. C **72**, 2100 (2012) [arXiv:1204.1258 [hep-ex]].

[16] G. Aad *et al.* (ATLAS Collaboration), Nucl. Phys. **B850**, 387 (2011) [arXiv:1104.3038 [hep-ex]].

[17] B. Abelev *et al.* (ALICE Collaboration), J. High Energy Phys. 11 (2012) 065 [arXiv:1205.5880 [hep-ex]].

[18] B. A. Kniehl, G. Kramer, I. Schienbein, and H. Spiesberger, Phys. Rev. D **71**, 014018 (2005) [hep-ph/0410289]; Eur. Phys. J. C **41**, 199 (2005) [hep-ph/0502194]; AIP Conf. Proc. **792**, 867 (2005) [hep-ph/0507068]; Phys. Rev. Lett. **96**, 012001 (2006) [hep-ph/0508129]; B. A. Kniehl, in *Proceedings of the 14th International Workshop on Deep Inelastic Scattering (DIS 2006)*, Tsukuba, Japan, 20–24 April 2006, edited by M. Kuze, K. Nagano, and K. Tokushuku (World Scientific, Singapore, 2007), p. 573 [hep-ph/0608122]; T. Kneesch, B. A. Kniehl, G. Kramer, and I. Schienbein, Nucl. Phys. **B799**, 34 (2008) [arXiv:0712.0481 [hep-ph]]; B. A. Kniehl, in *Proceedings of the XVI International Workshop on Deep-Inelastic Scattering and Related Subjects (DIS 2008)*, London, England, 7–11 April 2008, edited by R. Devenish und J. Ferrando (Science Wise Publishing, Amsterdam, 2008) [arXiv:0807.2215 [hep-ph]]; B. A. Kniehl, G. Kramer, I. Schienbein, and H. Spiesberger, Phys. Rev. D **79**, 094009 (2009) [arXiv:0901.4130 [hep-ph]]; Eur. Phys. J. C **62**, 365 (2009) [arXiv:0902.3166 [hep-ph]]; B. A. Kniehl, in *Proceedings of the XVII International Workshop on Deep-Inelastic Scattering and Related Subjects (DIS 2009)*, Madrid, Spain, 26–30 April 2009, edited by

C. Glasman and J. Terron (Science Wise Publishing, Amsterdam, 2009) [arXiv:0907.0184 [hep-ph]]; B. A. Kniehl, G. Kramer, and S. M. Moosavi Nejad, Nucl. Phys. **B862**, 720 (2012) [arXiv:1205.2528 [hep-ph]].

[19] B. A. Kniehl, G. Kramer, I. Schienbein, and H. Spiesberger, Phys. Rev. D **77**, 014011 (2008) [arXiv:0705.4392 [hep-ph]].

[20] B. A. Kniehl, G. Kramer, I. Schienbein, and H. Spiesberger, Phys. Rev. D **84**, 094026 (2011) [arXiv:1109.2472 [hep-ph]].

[21] A. Heister *et al.* (ALEPH Collaboration), Phys. Lett. B **512**, 30 (2001) [hep-ex/0106051].

[22] G. Abbiendi *et al.* (OPAL Collaboration), Eur. Phys. J. C **29**, 463 (2003) [hep-ex/0210031].

[23] K. Abe *et al.* (SLD Collaboration), Phys. Rev. Lett. **84**, 4300 (2000) [hep-ex/9912058]; Phys. Rev. D **65**, 092006 (2002); **66**, 079905(E) (2002) [hep-ex/0202031].

[24] P. M. Nadolsky, H.-L. Lai, Q.-H. Cao, J. Huston, J. Pumplin, D. Stump, W.-K. Tung, and C.-P. Yuan (CTEQ Collaboration), Phys. Rev. D **78**, 013004 (2008) [arXiv:0802.0007 [hep-ph]].

[25] V. Khachatryan *et al.* (CMS Collaboration), Phys. Rev. Lett. **106**, 112001 (2011) [arXiv:1101.0131 [hep-ex]]; S. Chatrchyan *et al.* (CMS Collaboration), *ibid.* **106**, 252001 (2011) [arXiv:1104.2892 [hep-ex]]; Phys. Rev. D **84**, 052008 (2011) [arXiv:1106.4048 [hep-ex]].

[26] V. Krey and K. R. S. Balaji, Phys. Rev. D **67**, 054011 (2003) [hep-ph/0209135].

[27] LHAPDF, the Les Houches Accord PDF Interface, URL: `http://projects.hepforge.org/lhapdf/pdfsets`.

[28] G. Alexander *et al.* (OPAL Collaboration), Phys. Lett. B **364**, 93 (1995).

[29] J. Beringer *et al.* (Particle Data Group Collaboration), Phys. Rev. D **86**, 010001 (2012).

[30] B. Aubert *et al.* (BaBar Collaboration), Phys. Rev. D **67**, 032002 (2003) [hep-ex/0207097].